(Ni$_{0.7}$Zn$_{0.3}$)Fe$_2$O$_4$/APTES-GO as An Eco-Friendly Catalyst for One-Pot Three-component Synthesis of 2-Amino-4*H*-chromene Derivatives

Fatemeh Janati[a],* [iD] , Sevda Ghanbarpoor[a] [iD] , Soghra Fathalipour[b] [iD]

[a]*Department of Chemistry, Payame Noor University, P.O Box: 19395-4697, Tehran, Iran. E-mail: fsjanati@gmail.com, fsjanati@pnu.ac.ir*
[b]*Shahid Bakeri high education center of Miandoab, Urmia University, Urmia, Iran*

Abstract: In this research, GO was modified with 3-aminopropyl triethoxysilane (APTES-GO), and then was mixed with prepared (Ni$_{0.7}$Zn$_{0.3}$) Fe$_2$O$_4$ to obtain (Ni$_{0.7}$Zn$_{0.3}$)Fe$_2$O$_4$/APTES-GO nanocomposite. The composite was characterized by FT-IR, XRD, SEM, and EDX. Results confirmed the modification of GO with APTES, and the presence of Ni, Zn, and face-centered cubic (FCC) structure of Fe$_2$O$_4$. Finally, composite was used as an eco-friendly catalyst in one-pot synthesis of 2-amino-4H-chromene via three-component reaction of malononitrile, aromatic aldehydes, and resorcinol. The obtained catalyst was recovered by an external magnetic field and reused several times without significant activity loss. Resulting 2-amino-4H-chromenes were purified and then characterized by FT-IR, ^{13}C NMR and ^{1}H NMR spectrums.

Keywords: 2-Amino-4*H*-chromene, Magnetic catalysts, Graphene oxide, Heterogeneous catalyst, 3-Aminopropyl triethoxysilane

1. Introduction

The 2-amino-4*H*-chromene and their derivatives have a significant impact in a variety of biological applications such as antiproliferative,[1] antimicrobial,[2] antitumor,[3] cancer therapy, sex pheromone,[4] and central nervous system.[5] Various methods have been proposed to prepare the 2-amino-4*H*-chromene by resorcinol, aldehydes, and malononitrile. [5-8] Different catalysts, such as cetyltrimethylammonium bromide (CTABr),[9] Bimetallic PdRu/graphene oxide,[10] piperazine-functionalized nickel ferrite NPs,[11] ferric hydrogen sulfate and Zr[12] have been used for the Knoevenagel reaction. Among used methods, the heterogeneous catalytic systems are suitable for the three-component synthesis of chromenes due to simple separation from the reaction mixture compared to other existing catalytic methods.[6, 11, 13] However, the design and preparation of a practical heterogeneous catalytic process still have many obstacles for researchers to achieve high efficacy. The spinel ferrites such as MFe$_2$O$_4$ (M: Zn, Ca, Ni, Mn) have attracted significant attention, owing to their magnetic/electric activities, stability, and comprehensive applications.[14-16] Furthermore, their magnetic properties lead to the facile isolation of the catalyst from the reaction mixture. However, the unprotected magnetic particles manifest high-degraded characteristics, resulting in more aggregation and instability.[17] Therefore, these particles are often protected on substrates with functional groups. Among different substrates, GO is recently used to adjust and immobilize the surface of the magnetic nanoparticles.[14-16] In this study, biocompatible magnetic nanocatalyst was synthesized from the loading of obtained (Ni$_{0.7}$Zn$_{0.3}$) Fe$_2$O$_4$ via ball mill reaction on (3-aminopropyl)triethoxysilane modified GO ((Ni$_{0.7}$Zn$_{0.3}$)Fe$_2$O$_4$/APTES-/GO). Resulting heterogeneous magnetic catalyst was utilized in one pot Knoevenagel condensation reaction for the synthesis of 2-amino-4*H*-chromene derivatives.

2. Results and Discussion

The XRD patterns of the (Ni$_{0.7}$Zn$_{0.3}$)Fe$_2$O$_4$ and (Ni$_{0.7}$Zn$_{0.3}$)Fe$_2$O$_4$/APTES-GO are shown in Figure 1. The peaks of phase (Ni$_{0.7}$Zn$_{0.3}$)Fe$_2$O$_4$ are marked using a black rhombus on the XRD patterns. In XRD pattern of (Ni$_{0.7}$Zn$_{0.3}$)Fe$_2$O$_4$, peaks at 2θ of 30.1, 35.5, 37.1, 43.5, 55.2, 58.1, 65.3, 72.2, and 74.1 related to XRD diffraction planes (220), (311), (222), (400), (511), (440), (531), (533) and (444) of Ni$_{0.7}$Zn$_{0.3}$Fe$_2$O$_4$ with face-centered cubic (FCC) structure (JCPDS card no. 8-02334).[16] In RD pattern of (Ni$_{0.7}$Zn$_{0.3}$)Fe$_2$O$_4$/APTES-GO, all peaks of (Ni$_{0.7}$Zn$_{0.3}$)Fe$_2$O$_4$ were appeared and only the high of peaks is lower than magnetic nanoparticles, which this can be related to the presence of APTES-GO. The other new peaks are related to the GO and APTES.[18, 19]
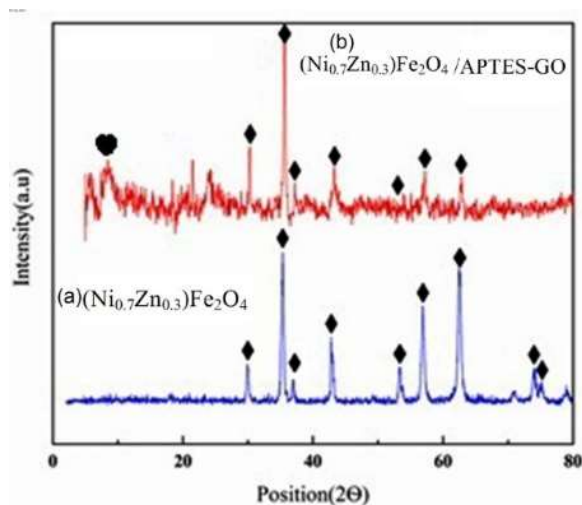
Figure 1. XRD patterns of (a) $(Ni_{0.7}Zn_{0.3})Fe_2O_4$; (b) $(Ni_{0.7}Zn_{0.3})Fe_2O_4/APTES-GO$.

SEM images of $(Ni_{0.7}Zn_{0.3})Fe_2O_4/APTES-GO$ were reported at different magnifications (Figure 2) to study the sample's morphology. As the SEM images show, spherical nanoparticles have been dispersed on GO sheets. Moreover, the related mapping EDS analysis was performed to investigate the uniformity of element distribution in the sample (Figure 3a). EDX analysis was also performed on the area marked with a yellow arrow in Figure 3a, which was reported in (Figure 3b).

The EDS spectra exhibit the presence of C, N, O, Fe, Zn, Ni, and Si elements in the $(Ni_{0.7}Zn_{0.3})Fe_2O_4/APTES-GO$ structure. Atomic percentage of these elements is almost 34%, 14%, 33%. 17%, 1.2%, and 0.73%, respectively.

Figure 2. SEM image of $(Ni_{0.7}Zn_{0.3})Fe_2O_4/APTES-GO$.

Element	Weight %	Atomic %
C	22.96	33.64
N	11.36	14.27
O	29.53	32.48
Si	26.94	16.88
Fe	3.81	1.2
Ni	2.43	0.73
Zn	2.98	0.8
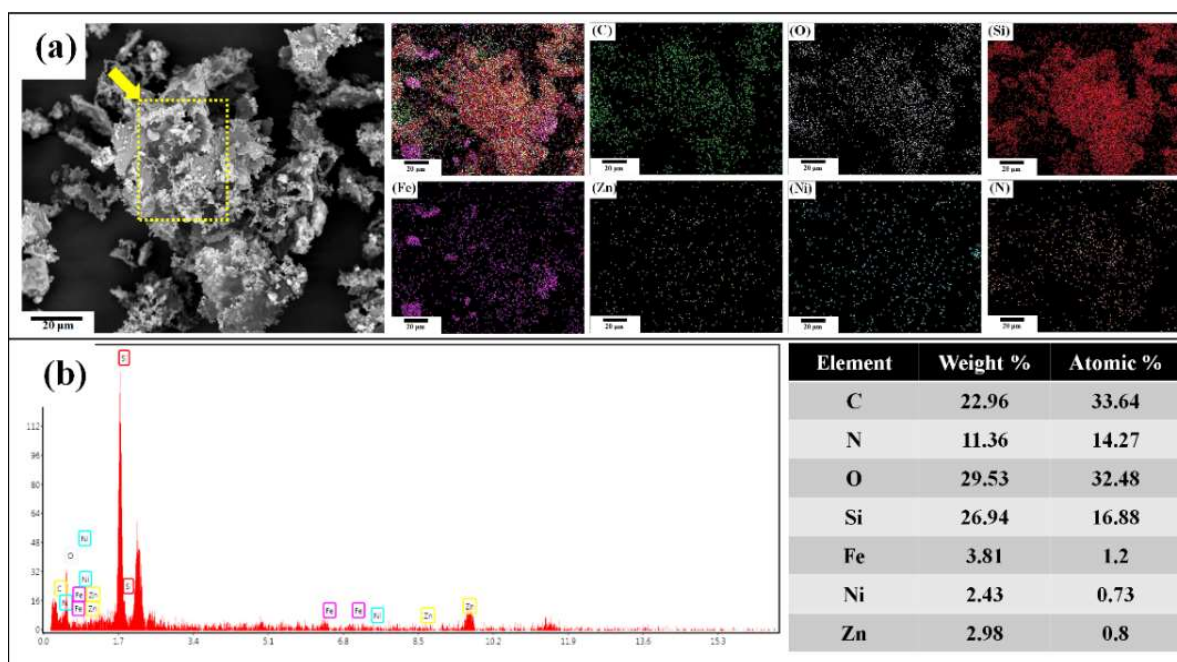
Figure 3. EDS analysis of $(Ni_{0.7}Zn_{0.3})Fe_2O_4/APTES-GO$.
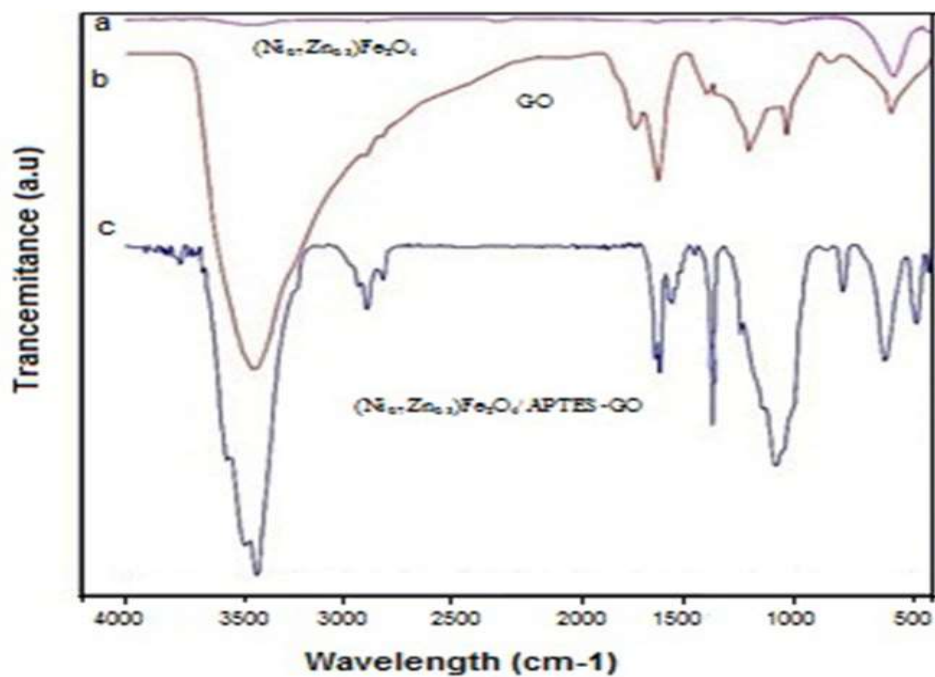
Figure 4. FT-IR spectra of $(Ni_{0.7}Zn_{0.3})Fe_2O_4$ (a), GO (b), and $(Ni_{0.7}Zn_{0.3})Fe_2O_4$/APTES-GO composite (c).

Figure 4 illustrates the FT-IR spectra of $(Ni_{0.7}Zn_{0.3})Fe_2O_4$, GO, and $(Ni_{0.7}Zn_{0.3})Fe_2O_4$/APTES-GO compounds. In Figure 4a, the strong peaks appeared near 576 cm^{-1} correspond to the characteristic peak of Ni-Zn ferrite, that Fe-O peak can also appear in the same area. In Figure 4b, the pure GO represents three peaks at 1060, 1641, and 3420 cm^{-1}, relating to the epoxy, carboxyl, and hydroxyl groups, respectively.[20] In Figure 4c, two peaks at 2863 and 2934 cm^{-1} correspond to the symmetric and asymmetric stretching modes of carbon-hydrogen bonds of CH_2-CH_2 groups with the NH_2 group.[21] Furthermore, two peaks at 801 and 1569 cm^{-1} attribute to the N-H out-of-plane bending vibration of the NH_2 group and the

symmetric N-H stretching band, respectively.[21] The appearance of two peaks at 1031 and 1109 cm^{-1} is related to the Si-O-C stretching vibration and Si-O-Si asymmetric stretching.[21, 22] Two broad bands at 3406 and 1620 cm^{-1} represent the hydroxide group and H-O-H bending vibrations of absorbed water. Additionally, the comparison between Figure 4a, Figure 4b, and Figure 4c describes the presence of the amino peak, and the stretching vibrations of C-C-O and C=C in Figure 4c, and this show the successful loading of $(Ni_{0.7}Zn_{0.3})Fe_2O_4$ on the APTES-GO.

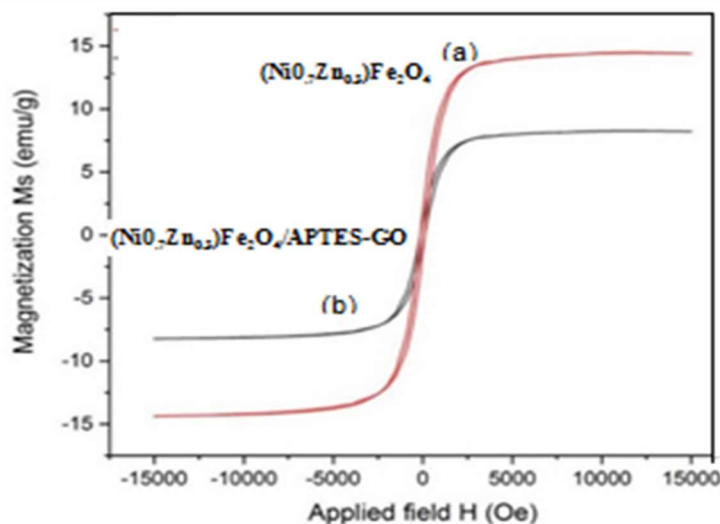**Figure 5.** VSM of $(Ni_{0.7}Zn_{0.3})Fe_2O_4$ (a) and $(Ni_{0.7}Zn_{0.3})Fe_2O_4$/APTES-GO composite (b).

Figure 5 shows the VSM results of $(Ni_{0.7}Zn_{0.3})Fe_2O_4$ and $(Ni_{0.7}Zn_{0.3})Fe_2O_4$/APTES-GO. The saturation magnetization amount of $(Ni_{0.7}Zn_{0.3})Fe_2O_4$ composite is 13.8 emu/g (Figure 5-a), which decreased to 10.8 emu/g after the loaded on APTES-GO, that this decreasing can be related to the presence of modified GO with APTES. Although the magnetite saturation decreased with loading of $(Ni_{0.7}Zn_{0.3})Fe_2O_4$ on APTES-GO surface, the magnetization of the final composite was still sufficient to separate the mixture using an external magnetic field.

According to the characterization, the catalyst could be used for the sequential cascade-type synthesis of 4*H*-chromene **(4)** scaffolds with biological activity selected. Therefore, various reaction parameters in the presence of the catalyst such as the solvent effect, the substrate, and the time of reaction have been investigated to optimize the synthesis procedure. The Knoevenagel condensation reaction of resorcinol **(1)** benzaldehyde **(2)**, and malononitrile **(3)** has been chosen as the reaction model (Scheme 1).
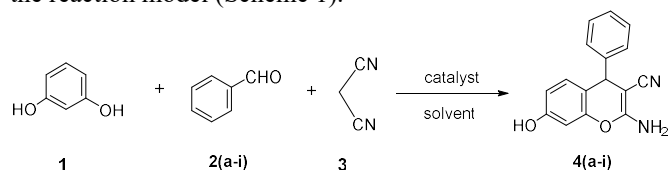
Scheme 1. The synthesis of 4*H*-chromene derivatives

The influence of various solvents was studied by replication the reaction with several solvents, and the corresponding results have been listed in Table 1.

Solvent plays a crucial role in the reaction rate and consequently the yield of the desired product of Knoevenagel condensation. Studies revealed that the polarity of the solvent is the most important parameter for the Knoevenagel condensation reaction. In contrast, water as polar green solvent was the only solvent candidate to favor this reaction with 90% yield compared to EtOH as the nearest polar competitor solvent with a yield of 80% in 30 min. On the other hand, the non-polar and aprotic solvents such as THF, CHCl₃, and n-Hexane display moderate product yield. Accordingly, water is the most favorable polar and protic solvents among the studied solvent for this reaction due to its strong hydrogen bonding with the catalyst than the other studied polar solvents. Therefore, this method is quite amenable and practical for the broad-scale synthesis of bioactive 2-amino-4*H*-chromene in the presence of water as a solvent.

Table 2 shows the effect of the catalyst amount on the rate and yield of synthesis of 4*H*-chromene derivatives and also, the comparison of this catalyst with the other catalysts. The results show that the rate and yield of reaction with our catalyst is higher than the others. To obtain the optimal amount of magnetic nanocatalyst, different amounts of nanocatalyst (5, 10, 15 and 20 mg) were used in water solvent under laboratory conditions (Table 2, Entries 5-8). According to the Table 2, increasing of the catalyst amount more than 15 mg, a significant effect did not show on the yield of the product. On

the other hand, reducing the amount of catalyst from 10 mg to 5 mg decrease the yield of reaction. Therefore, based on the results, maximum yield (i.e., 90%) at the short reaction time was achieved when 15 mg of $(Ni_{0.7}Zn_{0.3})Fe_2O_4$/APTES-GO was applied (Entry 7). The optimal amount of catalyst used in the synthesis of 4H-chromene derivatives is equal to 15 mg. After several screening tests with different amounts of the nanocatalyst, it was found that the Enhancing the amount of catalyst beyond 15-20 mg did not lead to any substantial progress in the product yield (Table 2, Entry 7,8). Whereas the lower amount of catalyst needed for the reaction from 10 mg to 5 mg led to reducing the efficiency of the reaction (Table 2, Entry 5 and 6). The effect of functional groups on the aryl aldehydes in the Knoevenagel condensation reaction catalyzed with $(Ni_{0.7}Zn_{0.3})Fe_2O_4$/APTES-GO was studied (Table 3). Both aldehydes substituted with the electron-donating groups and aldehydes substituted with the electron-withdrawing groups show 80-95% yields (Table 3) in the synthesis of 2-amino-3-cyano-7-hydroxy-4-aryl-4*H*-chromenes by Knoevenagel condensation reaction.

Table 1. Optimization of the reaction condition[a]

Entry	Solvent	Time (min)	Yield (%)
1	MeOH	30	75
2	Toluene	30	55
3	EtOH	30	80
4	H₂O	30	90
5	THF	30	50
6	CHCl₃	30	60
7	n-Hexane	30	25

[a]Reaction condition: benzaldehyde (1 mmol), malononitrile (1 mmol), resorcinol (1 mmol), and solvent (5 mL) over $(Ni_{0.7}Zn_{0.3})Fe_2O_4$/APTES-GO (15 mg) in room temperature.

Table 2. Effect of amounts of the catalyst[a]

| Entry	Catalyst (mg)	Time (min)	Yield (%a)
1	$(\alpha\text{-}Fe_2O_3)$-MCM-41-NH2-/30	120	45[23]
2	KF-Al₂O₃/30	600	Trace[23]
3	Without catalyst	60	35[23]
4	Fe₃O₄-GO/30	40	70
5	$(Ni_{0.7}Zn_{0.3})Fe_2O_4$/APTES-GO/5	30	90
6	$(Ni_{0.7}Zn_{0.3})Fe_2O_4$/APTES-GO/10	30	90
7	$(Ni_{0.7}Zn_{0.3})Fe_2O_4$/APTES-GO/15	25	90
8	$(Ni_{0.7}Zn_{0.3})Fe_2O_4$/APTES-GO/20	25	90

[a]Reaction condition: benzaldehyde (1 mmol), malononitrile (1 mmol), resorcinol (1 mmol), and water (5 mL) over $(Ni_{0.7}Zn_{0.3})Fe_2O_4$/APTES-GO in room temperature.

Comparatively, the reaction rate of aldehydes substituted with the electron-donating groups (4-CH₃, 4-CH₃O-, 3,4-(CH₃)₂O) is slower than aldehydes substituted with the electron-withdrawing groups (2-Cl, 4-Cl, 3-Nitro, 2-Nitro). The present procedure is compared with previous methods to indicate the advantages of $(Ni_{0.7}Zn_{0.3})Fe_2O_4$/APTES-GO magnetic catalyst in the synthesizing of 2-amino-4-phenyl-7-hydroxy-4*H*-chromene-3-carbonitrile. As clear from Table 3, the present work's privileges are probably evident regarding the common reaction yields in the chemical industry. The reusability and easy separation of the present catalyst is another dominant factor.

The mechanism relating to the condensation of various aldehydes, malononitrile, and resorcinol to prepare 2-amino-4H-chromene catalyzed by $(Ni_{0.7}Zn_{0.3})Fe_2O_4$/APTES-GO in the water has been given in Scheme 2. The first step of this condensation is the formation of the Knoevenagel product from aryl aldehyde and malononitrile (intermediate **I**). Acidic and amine functional groups on the surface of f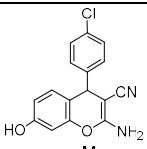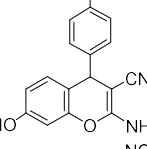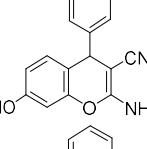unctionali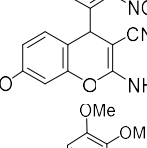zed GO can be cataly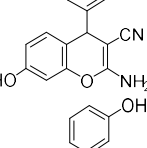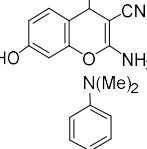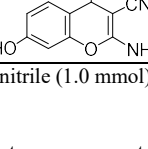st the removal of proton from the malononitrile,[23] and on the other hand, the presence of transition metals in this compound can act as a Lewis acid, [24] so catalyst the reaction, and gives the malononitrile anion. Then, the malononitrile anion reacts with the carbonyl group of substituted aldehydes followed by the hydrolysis of the intermediate in the solvent phase, which finally yields the product.
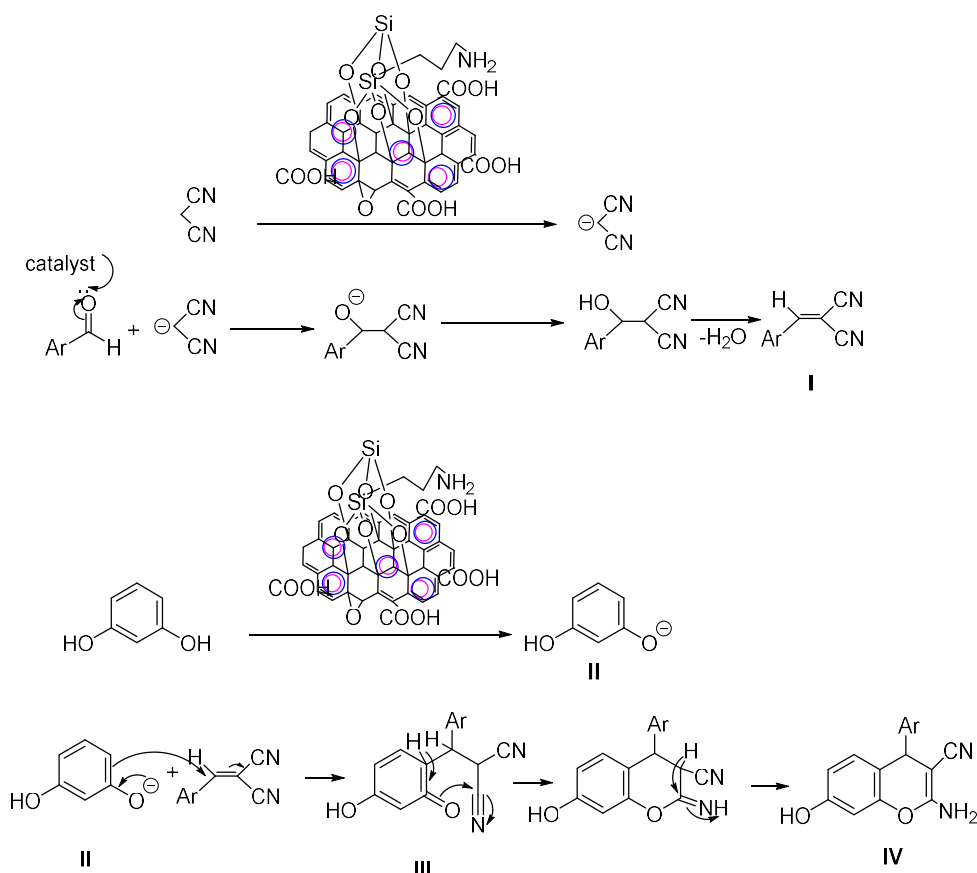
Scheme 2. A plausible mechanism for the synthesis of 2-amino-4H-chromenes

Table 3. Broad substrate scope for 2-Amino-3-cyano-7-hydroxy-4-aryl-4H-chromenes synthesis[a]

Entry	Ar	Product	T (min)	Yield (%)	Mp (ºC)	
					Found	Reported (lit)
a	C_6H_5		25	90	231-233	234-236[25]
b	2-Cl-C_6H_4		35	92	93-92	96-98[26]

Entry	Ar	Product	T (min)	Yield (%)	Mp (°C) Found	Mp (°C) Reported (lit)
c	4-Cl-C_6H_4		25	95	158-160	160-162[26]
d	4-Me-C_6H_4		30	89	180-182	184-186[26]
e	3-NO_2-C_6H_4		25	95	189-191	188-192[27]
f	2-NO_2-C_6H_4		20	88	162-164	162-163[28]
g	3,4-MeO-C_6H_4		40	85	216-217	215-217[27]
h	3-OH-C_6H_4		35	90	210-214	215-217[24]
i	4-(Me)2N-C_6H_4CHO		40	88	194-196	193-195[28]

[a]Reaction condition: Arylaldehyde (1 mmol), malononitrile (1.0 mmol), resorcinol (1 mmol), water (5 mL), and $(Ni_{0.7}Zn_{0.3})Fe_2O_4$/APTES-GO(15mg) in room temperature

After completion of the reaction, the catalyst was separated by the external magnetic, washed with the ethanol/water, dried at 60 °C in a vacuum oven, and finally reused in the reaction. The recycled catalyst was utilized for three-time in reactions without loss of conversion. The activity of the catalyst decreased after 3 times recovery.

Spectra data of the representative compounds
Entry 1: 2-Amino-4-phenyl-7-hydroxy-4*H*-chromene-3-carbonitrile: Yield: 90%; m.p: 231-233 °C; FT-IR (KBr, cm^{-1}): 1593, 1622, 2198, 3363, 342, ^{1}H-NMR (300 MHz, DMSO-d_6, δ/ppm): 9.68 (s, 1H, OH), 6.85(s, 2H, NH_2), 6.40-7.31 (m, 8H, Ar-H), 4.61(s, 1H, H-4), ^{13}C NMR (100 MHz, DMSO-d6): δ 56.32, 102.71, 112.96, 113.37, 113.66, 121.01, 128.23, 129.04, 129.75, 130.31, 130.38, 131.72, 145.79, 149.29, 157.69, 160.72.

Entry 2: 2-Amino-4-(4-chlorophenyl)-7-hydro-xy-4*H*-chromene-3-carbonitrile: Yield: 92%; m.p: 157-160 °C; IR (KBr, cm^{-1}): 1589, 1642, 3335, 3450, ^{1}H NMR (300 MHz, DMSO- d_6, δ/ppm): 9.68 (s, 1H, OH), 6.85 (s, 2H, NH_2), 6.37-7.33 (m, 7H, Ar-H), 4.62 (s, 1H, H-4), ^{13}C NMR (100 MHz, DMSO-d6): δ 56.09, 102.59, 112.72, 112.97, 113.32, 114.64, 121.25, 125.87, 128.69, 130.93, 131.17, 138.74, 149.21, 158.02, 158.32, 160.44.

Entry 3: 2-Amino-4-(2-chlorophenyl)-7-hydroxy-4*H*-chromene-3-carbonitrile: Yield: 95%; m.p: 93-95 °C; IR (KBr, cm^{-1}): 1588, 1654, 2192, 3335, 3419, ^{1}H NMR (300 MHz, DMSO-d_6, δ/ppm): 9.68 (s, 1H, OH), 6.85 (s, 2H, NH_2), 6.37-7.33 (m, 7H, Ar-H), 4.62 (s, 1H, H-4), ^{13}C NMR (100 MHz, DMSO-d6): δ 55.04, 101.56, 110.78, 112.90, 114.38, 114.52, 121.19, 126.47, 128.89, 129.92, 130.39, 136.91, 147.26, 156.48, 155.40, 161.51.

Entry 4: 2-Amino-4-(4-methylphenyl)-7-hydroxy-4H-chromene-3-carbonitrile: Yield: 89%; m.p: 181-183 °C; IR (KBr, cm^{-1}): 1510; 1615, 2191, 3369, 3409, ^{1}H NMR (300 MHz, DMSO-d$_6$, δ/ppm): 9.62 (s, 1H, OH), 6.81 (s, 2H, NH$_2$), 6.30-7.10 (m, 7H, Ar-H), 4.56 (s, 1H, H-4), 2.24 (s, 3H, CH$_3$), ^{13}C NMR (100 MHz, DMSO-d6): δ 55.62, 56.47, 102.77, 112.73, 113.82, 121.02, 128.64, 129.65, 130.22, 131.02, 143.06, 149.15, 156.63, 159.83, 161.70.

Entry 5: 2-Amino-4-(3-nitrophenyl)-7-hydroxy-4H-chromene-3-carbonitrile: Yield: 95%; m.p: 162-164 °C; IR (KBr, cm^{-1}): 1591/25, 1688, 2185, 3343, 3409; ^{1}H NMR (300 MHz, DMSO-d$_6$, δ/ppm): 9.80 (s, 1H, OH), 7.0 (s, 2H, NH$_2$), 6.43-7.86 (m, 7H, Ar-H), 5.14 (s, 1H, H-4), ^{13}C NMR (100 MHz, DMSO-d6): δ 55.42, 56.22, 102.41, 113.16, 113.32, 113.96, 121.12, 127.23, 128.34, 128.67, 130.43, 130.57, 138.68, 148.79, 157.39, 158.61, 160.40.

Entry 6: 2-Amino-4-(2-nitrophenyl)-7-hydroxy-4H-chromene-3-carbonitrile: Yield: 88%; m.p: 189-191 °C; IR (KBr, cm^{-1}): 1589, 1642, 2194, 3329, 3438, ^{1}H NMR (300 MHz, DMSO-d$_6$, δ/ppm): 9.77 (s, 1H, OH), 7.02 (s, 2H, NH$_2$), 6.44-8.10 (m, 7H, Ar-H), 4.90 (s, 1H, H-4), ^{13}C NMR (100 MHz, DMSO-d6): δ 56.63, 102.72, 112.71, 112.91, 113.83, 113.97, 121.13, 121.63, 129.75, 129.95, 130.37, 142.04, 149.35, 155.62, 159.94, 160.67.

Entry 7: 2-Amino-4-(3,4-dimethoxyphenyl)-7-hydroxy-4H-chromene-3-carbonitrile: Yield: 85%; m.p: 216-217 °C; IR (KBr, cm^{-1}): 1586, 1645, 2186, 3350, 3447; ^{1}H NMR (300 MHz, DMSO-d$_6$, δ/ppm): 9.66 (s, 1H, OH), 6.45-7.12 (m, 6H, Ar-H), 6.38 (s, 2H, NH$_2$), 4.55 (s, 1H, H-4), 3.69 (s, 6H, OCH$_3$), ^{13}C NMR (100 MHz, CDCl$_3$+ DMSO-d6); δ 41.1, 55.8, 55.9, 60.0, 111.1, 117.3, 120.4, 120.9, 123.2, 124.3, 126.2, 126.5, 126.7, 127.7, 133.2, 137.4, 143.2, 148.1, 149.1, 159.4.

Entry 8: 2-Amino-4-(3-hydroxyphenyl)-7-hydroxy-4H-chromene-3-carbonitrile: Yield: 90%; m.p: 210-214 °C; IR (KBr, cm^{-1}): 1506, 1600, 2192, 3360, 3427; ^{1}H NMR (300 MHz, DMSO-d$_6$, δ/ppm): 9.68 (s, 1H, OH), 6.31-7.08 (m, 7H, Ar-H), 6.87 (s, 2H, NH$_2$), 4.49 (s, 1H, H-4), ^{13}C NMR (100 MHz, DMSO-d6): δ 57.04, 102.57, 112.79, 112.93, 114.38, 114.52, 121.19, 126.47, 128.89, 129.92, 130.39, 138.94, 149.22, 157.42, 158.42, 160.54.

Entry 9: 2-Amino-4-(4-dimethylaminophenyl)-7-hydroxy-4H-chromene-3-carbonitrile: Yield: 88%; m.p: 194-196 °C; IR (KBr, cm^{-1}): 1583, 1638, 2190, 3340, 3437, ^{1}H NMR (300 MHz, DMSO-d$_6$, δ/ppm): 9.66 (s, 1H, OH), 6.37-6.97 (m, 7H, Ar-H), 6.72 (s, 2H, NH$_2$), 4.46 (s, 1H, H-4), 2.84 (s, 6H, N(CH$_3$)$_2$), ^{13}C NMR (100 MHz, DMSO-d6): δ 34.27, 53.86, 102.82, 106.74, 109.58, 110.32, 112.74, 120.96, 130.02, 146.79, 149.56, 151.40, 155.60, 157.82, 161.33.

3. Experimental

Preparation of (Ni$_{0.7}$Zn$_{0.3}$)Fe$_2$O$_4$

The sample powder was ground by a ball mill with a rate of 150 rpm and the ratio of ball to powder 10:1 for one hour for mixing and calcined for four hours at a temperature of 1000 °C. The milled powder was pressed under a uniaxial pressure of 100 MPa to form 2 cm diameter and 1 cm thick tablets and heated up to 60 °C for 24 h. The samples were sintered at a temperature of 1200 °C for two hours. The disc-shaped sample was ground in a ceramic mortar, and for further crushing, the ball mill with 300 rpm and the ratio of ball to powder 10:1 has been used for ten hours. The phase identification was carried out with X-ray diffraction (Rigaku D/max 2500 PC diffractometer and Cu-Kα radiation).

Synthesis of GO and APTES/GO

The GO was prepared from natural graphite powder through a modified Hummers' method [24], in which 0.5 g of graphite was added to 12 mL of the concentrated H$_2$SO$_4$ (98% wt.). The mix was mechanically stirred for 20h at room temperature. Additionally, 50 mg of sodium nitrate was added to the mixture and stirred for 2510 to prevent oxidation. The mixture was then held under 4 °C in an ice bath. Simultaneously, 1.5 g of KMnO$_4$ was added into the mixed solution and stirred for 1.5 h, and 10 mLH$_2$O$_2$ (30%) and 125 mL distilled water were added to the mixture at room temperature. After 15 min of stirring, a bright yellow solution was obtained. Finally, the solution was precipitated for 10 h, and the products were collected by centrifugation. Subsequently, the GO powders were washed with 10% hydrochloric acid and distilled water three times and then dispersed in the distilled water to achieve a stable brown solution. The GO-containing solution was filtered, dried at 55 °C in a vacuum oven overnight, and ground into powder. Then, 0.5 g of GO was dispersed in 100 mL of ethyl alcohol by sonicating for 1 h. The solution was mixed with 2 mL of APTES and magnetically stirred for 5 h at 75 °C. Finally, the solid product was then washed with ethyl alcohol and water to remove excess aminopropyl triethoxysilane, and the washing process was followed by acetone. The APTES-GO was dried in a vacuum oven for 12 h at 60 °C and ground into a powder [25].

Preparation of magnetic (Ni$_{0.7}$Zn$_{0.3}$)-Fe$_2$O$_4$/APTES/GO composite

Homogenous aqueous APTES/GO has been prepared by dispersion of 0.3 g of APTES/GO in 100 mL double-distilled water and sonication for 1 h and 0.2 g of (Ni$_{0.7}$Zn$_{0.3}$)Fe$_2$O$_4$ was added to the mixture and stirred vigorously for six h at room temperature. The resulting (Ni$_{0.7}$Zn$_{0.3}$)Fe$_2$O$_4$/GO-/APTES powder was separated by an external magnetic field, washed with distilled water/ethyl alcohol, and dried at 50 °C in a vacuum oven overnight. Scheme 3 displays the synthesizing process of the (Ni$_{0.7}$Zn$_{0.3}$)Fe$_2$O$_4$/APTES/GO.

Preparation of the 2-amino-3-cyano-4*H***-chromenes**

A mixture of aryl-aldehyde (1 mmol), resorcinol (1 mmol), malononitrile (1 mmol), and $(Ni_{0.7}Zn_{0.3})Fe_2O_4$/APTES-GO composite (15 mg) was added to 5 mL H_2O/EtOH and stirred at 50 °C. A TLC test (ethyl acetate: n-hexane 1:1) monitored the reaction progress. The condensation reaction product was separated using ethyl acetate. Finally, the pure product was obtained through recrystallization from the EtOH.
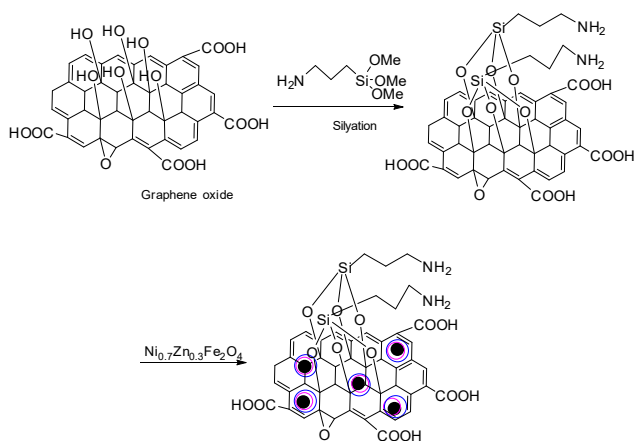
Scheme 3. Synthesis of catalyst $(Ni_{0.7}Zn_{0.3})Fe_2O_4$/GO/APTES

4. Conclusions

A novel facile electrostatic self-assembly method has been developed to modify the $(Ni_{0.7}Zn_{0.3})$ Fe_2O_4 magnetic functional catalyst particles uniformly on the surface of the GO sheet developed. The prepared $(Ni_{0.7}Zn_{0.3})Fe_2O_4$/GO-APTES hybrid was further presented as highly active heterogeneous catalysts in one-pot cascade synthesis of 2-amino-4*H*-chromene derivatives proceeded efficiently in water as a polar and protic solvent. The reaction conditions were mild, with excellent yields of products. The developed sustainable and environmentally friendly process did not involve hazardous organic solvents and high temperatures.

Declaration of Interests

There are no conflicts to declare.

Author(s) ID

Fatemeh Janati* (iD): 0000-0002-7475-9365.
Soghra Fathalipour (iD): 0000000165488121

References

1. H. A. Elshemy, M. A. Zaki, A. M. Mahmoud, S. I. Khan, A. G. Chittiboyina, A. M. Kamal, *Bioorg. Chem.,* **2022**, *118*, 105475.

2. R. Beldi, N. Aimene, B. Barhouchi, B. Zouchoune, R. Boulcina, *COCAT*, **2023**, *10*, 263-275.

3. P. G. de Abrantes, P. G. de Abrantes, D. A. dos Santos Silva, R. R. Magalhães, P. B. N. da Silva, G. C. G. Militão, R. P. B. de Menezes, L. Scotti, M. T. Scotti, J. A. Vale, *Med. Chem. Res.*, **2023**, *32*, 2234-2244.

4. V. T. Tonape, A. D. Kamath, K. Kamanna, *COCAT*, **2023**, *10*, 34-57.

5. K. Kantharaju, S. Y. Khatavi, *Asian J. Chem.*, **2018**, *30*, 1496-1502.

6. S. Akocak, B. Şen, N. Lolak, A. Şavk, M. Koca, S. Kuzu, F. Şen, *Nano-Struct. Nano-Objects*, **2017**, *11*, 25-31.

7. J. Safari, L. Javadian, *Ultrason. Sonochem.*, **2015**, *22*, 341-348.

8. F. Mohamadpour, *Monatsh. fur Chem.*, **2021**, *152*, 507-512.

9. T. -S. Jin, J. -C. Xiao, S. -J. Wang, T. -S. Li, *Ultrason. Sonochem.*, **2004**, *11*, 393-397.

10. B. Şen, N. Lolak, Ö. Paralı, M. Koca, A. Şavk, S. Akocak, F. Şen, *Nano-Struct. Nano-Objects,* **2017**, *12*, 33-40.

11. B. Pourhasan, A. Mohammadi-Nejad, *J. Chin. Chem. Soc.*, **2019**, *66*, 1356-1362.

12. H. Eshghi, S. Damavandi, G. Zohuri, *Synth. React. Inorg. Met.*, **2011**, *41*, 1067-1073.

13. R. Ferdousian, F. K. Behbahani, B. Mohtat, *Mol. Divers.*, **2022**, *26*, 3295-3307.

14. R. Bhattacharyya, O. Prakash, S. Roy, A. P. Singh, T. K. Bhattacharya, P. Maiti, S. Bhattacharyya, S. Das, *Sci. Rep.*, **2019**, *9*, 12111.

15. S. Gupta, S. K. Sharma, D. Pradhan, N. -H. Tai, *Compos. Part A Appl. Sci. Manuf.*, **2019**, *123*, 232-241.

16. G. R. Gordani, M. R. L. Estarki, M. Danesh, E. Kiani, M. Tavoosi, *Ceram. Int.*, **2022**, *48*, 3059-3069.

17. K. C. Souza, N. D. Mohallem, E. M. Sousa, *J. Solgel. Sci. Technol.*, **2010**, *53*, 418-427.

18. S. Fathalipour, S. Pourbeyram, S. C. Miandoab, *J. Iran. Chem. Soc.*, **2023**, *20*, 1395-1403.

19. Y. Li, H. Chen, J. Wu, Q. He, Y. Li, W. Yang, Y. Zhou, *Appl. Surf. Sci.*, **2018**, *447*, 393-400.

20. S. Pourbeyram, S. Fathalipour, B. Rashidzadeh, H. Firuzmand, B. Rahimi, *Environ. Sci.: Water Res.*, **2023**, *9*, 3355-3365.

21. S. Fathalipour, A. Zolali, B. Najafpour, S. Pourbeyram, M. Zirak, *Inorg. Nano-Met.*, **2021**, *51*, 47-54.

22. S. Fathalipour, M. Mardi, *Mater. Sci. Eng. C*, **2017**, *79*, 55-65.

23. S. Rostamizadeh, A. Hemmasi, N. Zekri, *Nanochem. Res.*, **2017**, *2*, 29-41.

24. J. Safari, Z. Zarnegar, M. Heydarian, *Bull. Chem. Soc. Jpn*, **2012**, *85*, 1332-1338.

25. A. Shestopalov, Y. M. Emelianova, V. Nesterov, *Russ. Chem. Bull.*, **2003**, *52*, 1164-1171.

26. K. Gong, H. L. Wang, J. Luo, Z. L. Liu, *J. Heterocycl. Chem.*, **2009**, *46*, 1145-1150.

27. S. R. Kale, S. S. Kahandal, A. S. Burange, M. B. Gawande, R. V. Jayaram, *Catal. Sci. Technol.*, **2013**, *3*, 2050-2056.

28. S. K. Sharma, P. A. Parikh, R. V. Jasra, *J. Mol. Catal. A Chem.*, **2007**, *278*, 135-144.